RSC Advances

PAPER

View Article Online
View Journal | View Issue

Cite this: *RSC Adv.*, 2021, **11**, 26992

Facile fabrication of superhydrophobic polyester fabric based on rapid oxidation polymerization of dopamine for oil–water separation

Ailing Xie, Boan Wang, Xinpeng Chen, Yahui Wang, Yirong Wang, Xiaowei Zhu, Tieling Xing * and Guoqiang Chen

Through the special chemical structure of dopamine (DA), superhydrophobic polyester (PET) fabric was fabricated by introducing the low surface energy substance hexadecyltrimethoxysilane (HDS) into the PET fabric and chelating Fe ions with phenolic hydroxyl groups of polydopamine (PDA) to form a rough surface. The water contact angle (WCA) of the prepared PDA/Fe/HDS PET fabric was higher than 160° and the scrolling angle (SA) was lower than 2.09°. The excellent adhesion property of polydopamine (PDA) on the substrate is helpful to improve the stability of superhydrophobic PDA/Fe/HDS PET fabric. The tests results showed that the modified PET fabric maintains excellent mechanical properties. Its superhydrophobic property had good stability and durability in the harsh environment of washing, mechanical friction, UV irradiation, seawater immersion, acid–base and organic reagents erosion. The PDA/Fe/HDS PET fabric also had good self-cleaning and oil–water separation properties. It still had good oil–water separation performance after repeated use for 25 times, and the separation efficiency was more than 95%. The preparation method was facile, the treatment time can be shortened, the cost of the modified substrate was low, and fluorine-free substances were used in the process. This work provides a new way to expand the added value of PET fabrics and develop durable superhydrophobic fabrics in practical application.

Received 5th July 2021
Accepted 31st July 2021

DOI: 10.1039/d1ra05167a

rsc.li/rsc-advances

Introduction

In the 21st century, the PET industry has made great progress. Due to its low price, excellent performance, easy washing and quick drying, it has become one of the most popular textile raw materials. Therefore, the functional finishing of PET fabric has become a research hotspot for researchers. In general, the solid–liquid WCA on the surface of this material is greater than 150°, and the SA is less than 10°.[1–3] Superhydrophobic PET fabric has outstanding self-cleaning, anti-fouling, anti-fogging, anti-icing, drag reduction and anti-corrosion functions,[4–7] and has important application values in industry, military, biomedicine and other fields. The idea to prepare superhydrophobic fabrics is to introduce low surface energy substances to reduce the surface tension of the fabric, and to generate nanoparticles on the surface of the fabric or etch them chemically or physically to construct a structure with a micro/nano rough structure similar to the lotus leaf surface. Therefore, researchers have adopted different strategies,[2] for example, by chemical vapor deposition,[3] sol–gel coating[4,5] and other methods to introduce fluorinating agents[8–13] and other low surface energy substances into the fabric, or using nanoparticle *in situ* growth,[14] chemical etching[15] or plasma etching[16,17] to endow the fabric surface with a micro/nano-level rough structure to achieve the superhydrophobic aim. However, the operations of these methods are complicated, or the reagent used is not environmentally friendly, and the prepared superhydrophobic material has poor stability, which seriously hinders practical application.[18]

Marine mussels have attracted widespread attention due to their excellent bio-adhesion. Mussels can adhere to almost all types of substrates in humid environments by secreting adhesion proteins.[19–22] Mucus proteins secreted by mussels mainly include mfp-1, mfp-2, mfp-3, mfp-4, mfp-5, and mfp-6.[23–25] Among them, mfp-3 and mfp-5 are the keys to interface adhesion. When contacting with a hydrophobic surface, mucins will expose an indole or benzene ring structure to form strong hydrophobic interactions with the surface, and studies show that their interaction with hydrophobic surfaces is much greater than with hydrophilic surfaces.[26–28] The modified substrate can be firmly combined with dopamine polymer by simple dip-coating in dopamine aqueous solution, which greatly improves the mechanical stability of the modified material.[29–32] At the same time, dopamine has active functional groups such as amino and phenolic hydroxyl groups, which can

College of Textile and Clothing Engineering, Jiangsu Engineering Research Center of Textile Dyeing and Printing for Energy Conservation, Discharge Reduction and Cleaner Production (ERC), Soochow University, No. 199, Renai Road, Suzhou 215123, China. E-mail: xingtieling@suda.edu.cn

produce a variety of chemical reactions, providing a reaction platform for the second modification of the substrate.

Dopamine is a non-toxic, environmentally friendly and highly adaptable substance. There are many reports about the application of dopamine in preparation of superhydrophobic fabrics. The traditional self-polymerization of dopamine under alkaline environment was used to modify the fabric,[33,34] and the introduction of fluorine-containing low surface energy substances can rapidly endow the fabric with superhydrophobic property.[35] The problem of these methods is that the preparation process is time consuming or the chemical used is not environmentally friendly. Therefore, a simple and pollution-free superhydrophobic preparation method with good stability is an urgent requirement.

In this paper, a simple, rapid and environmentally friendly preparation method of superhydrophobic PET fabrics was introduced. By using the excellent adhesion property of dopamine, low surface energy substance HDS was introduced to the surface of PET, and metal ions were chelated on the surface to form a rough convex and waxy "lotus leaf" like surface, and the superhydrophobic PET fabric was prepared. The basic principle of the reaction is as follows: dopamine acts as a ligand to form a stable dopamine/metal complex with metal ions as the center (Fig. 1a),[36–39] which forms nanoparticles on the surface of PET fabric. At the same time, the alkoxy group at one end of the molecular structure of silane coupling agent is hydrolyzed to silanol group, which is dehydrated and condensed to form oligosiloxane containing silanol group. It can form a hydrogen bond with a phenol hydroxyl group in the molecular structure of DA, and forms a covalent bond with PDA during the heating process (Fig. 1b). Under the catalysis of oxidants, DA molecules rapidly polymerize to form a network structure of polydopamine macromolecules (Fig. 1c),[40,41] which covers the surface of the fabric. Therefore, nano-scale particles were formed on the surface of PET fabric under the action of PDA, and the surface energy of the fabric was greatly reduced due to the introduction of HDS, and PDA/Fe/HDS PET fabric was prepared. The schematic of preparation of superhydrophobic PET fabric is shown in Fig. 1.

The surface morphology and chemical compositions of the PDA/Fe/HDS PET fabric were observed by SEM, AFM, EDS, XPS. The mechanical stability and stability in seawater, acid, alkali and organic solutions were further tested to simulate the durability of superhydrophobic PET fabric in complex marine environment. The results show that PDA/Fe/HDS PET fabric has excellent and stable superhydrophobic properties, indicating that this method has broad application prospects in the modification of superhydrophobic polyester, and providing a research basis for the industrial preparation of superhydrophobic PET fabric.

Experimental section

Materials

The polyester fabric (plain fabric, 89 g m^{-2}, warp density: 40 threads per cm; weft density: 27 threads per cm) was purchased from the market. Dopamine hydrochloride (98.5% purity) was purchased from Yuanye Biotechnology Co., Ltd., Shanghai, China. Hexadecyltrimethoxysilane, sodium perborate tetrahydrate and ferrous sulfate heptahydrate were purchased from

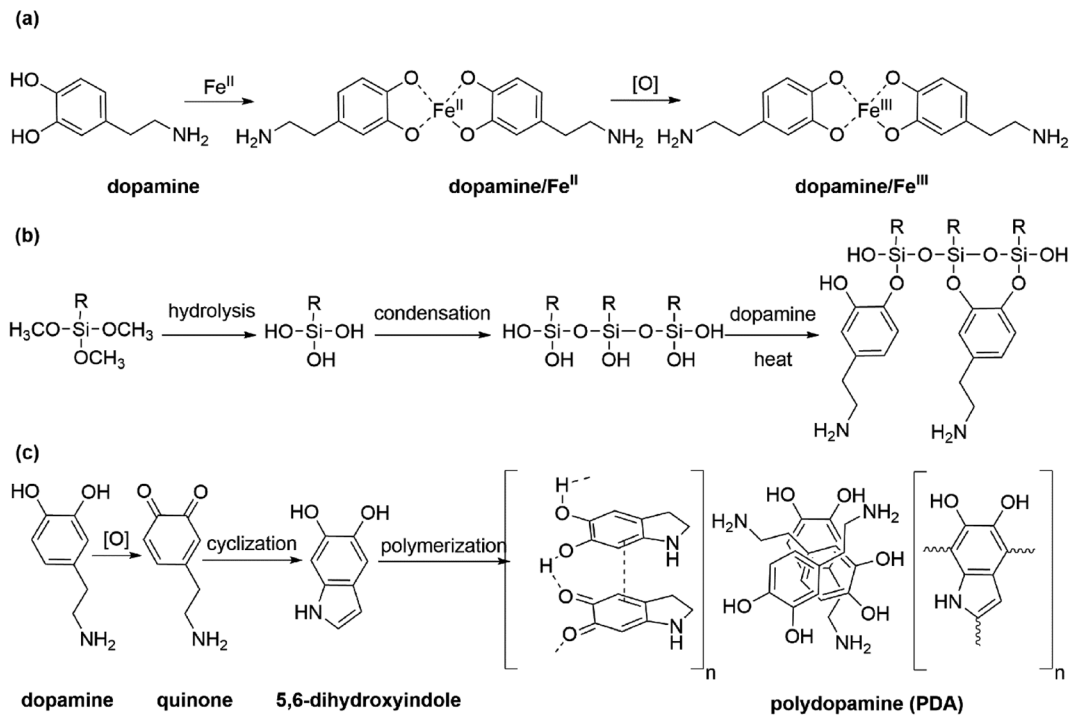

Fig. 1 Schematic of (a) dopamine chelated ions, (b) dopamine formed covalent bonds with long-chain alkyl siloxane and (c) the possible oxidative polymerization mechanism of PDA on the PET fabric.

Shanghai Aladdin Biochemical Technology Co., Ltd., Shanghai, China. All other chemicals were of analytical reagent grade and were used without further purification.

Fabrication of superhydrophobic polyester fabrics

The polyester fabric was immersed in a mixed solution containing 2 g L^{-1} dopamine, 0.72 mmol L^{-1} $FeSO_4 \cdot 7H_2O$ and 150 μL L^{-1} HDS, and the solution was shaken at 70 °C for 50 min. It is important to add 2 mmol L^{-1} sodium perborate tetrahydrate after 20 min of reaction. Finally, the fabric was washed with flowing water and dried in an oven at 60 °C. The schematic illustration of preparation of superhydrophobic PET fabric is shown in Fig. 2.

Characterization and measurements

The surface morphology of PET fabric was observed using a field emission scanning electron microscope (FESEM, Hitachi S-4800) at 3.0 kV. The Hitachi TM 3030 desktop scanning electron microscope (Hitachi Ltd., Tokyo, Japan) was used to observe the elemental mapping of the surface morphology of polyester fabrics in a vacuum with an accelerating voltage of 15 kV. The surface topography and roughness of the fabric were determined by an atomic force microscope (AFM, Multimode 8, Bruker Company). The surface element content of polyester samples was analyzed by Thermo Scientific K-Alpha$^+$ X-ray photoelectron spectroscopy (Thermo Fisher Scientific Co., Ltd., Waltham, MA, USA) using an Al Kα X-ray source (1486.6 eV). Surface-sensitive attenuated total reflection Fourier transform infrared (ATR-FTIR) spectra were carried out with Nicolet 5700 instrument. The water contact angle (WCA) and scrolling angle (SA) of the fabric samples were measured using Kruss DSA 100 (Kruss Company, Germany) instrument. The volume of the water droplets in WCA and SA measurements were 6 μL and 10 μL respectively, and the results were the average of five measurements.

Mechanical stability test

The INSTRON-3365 material testing machine (American INSTRON Company, Norwood, MA, USA) was used to test the tensile fracture strength of the fabric. The breaking strength and elongation at break of samples were tested according to ISO 13934-2013. The samples size was 30 cm × 5 cm, and the clamping length was 20 cm, and the stretching speed was 100 mm min^{-1}.

The washing stability test

The washing stability test and the Gray Scale rating were carried out according to AATCC 61-2006 standard method. In one washing cycle, the PDA/Fe/HDS PET fabric was put into 200 mL solution containing 0.37% detergent (special saponin slice for Shanghai textile test, Shanghai Textile Industry Technology Supervision Institute) and then washed using Wash Tec-P Fastness Tester (Roaches International, UK) with 10 steel balls at 40 °C for 45 min. The samples before and after washing were compared with the grey sample card (in accordance with ISO 105/A03 1993 standard). The staining fastness and fading fastness were obtained under the D65 light source and 10° observation angles.

The abrasion and UV irradiation stability tests

A Martindale abrasion tester (YG401G, Ningbo Textile Instrument Co., Ltd. China) was used to further test the abrasion resistance of the modified fabric based on ISO12947-4. The UV irradiation stability was tested at 60 °C for 4 h, 8 h, 12 h, 16 h, 20 h, 24 h using Accelerated Weathering Tester (340 Lamp, QUV/spray, Q-Lab, USA).

The seawater resistance stability test

The prepared superhydrophobic PET fabric will suffer seawater erosion when dealing with oil spills at sea. According to the standard of ISO 105 E02:2013 (E), Color Fastness Meter for

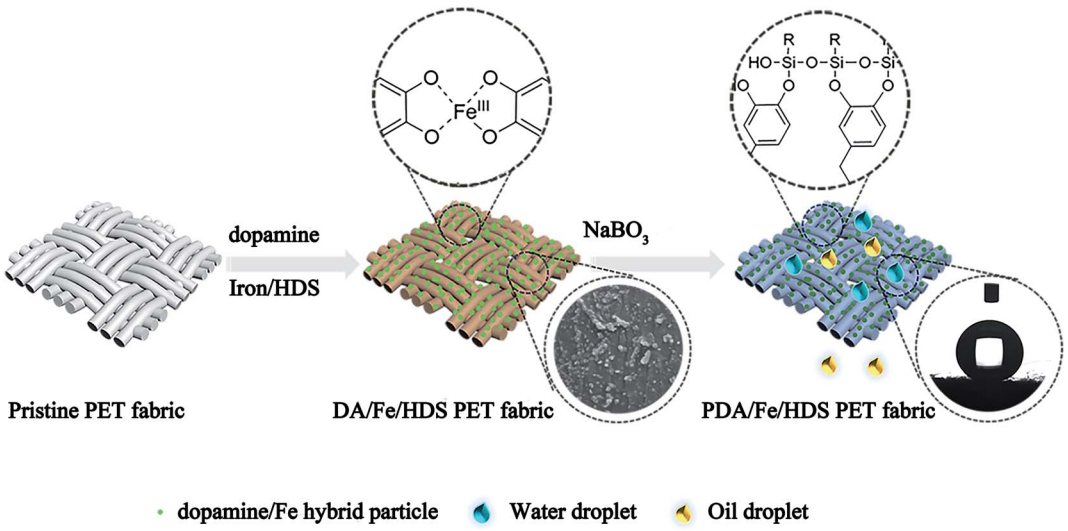

Fig. 2 Schematic of preparation of superhydrophobic PET fabric.

Perspiration (YG631, Nantong Hongda Experimental Instrument Co., Ltd., China) was used to test the seawater resistance stability of the fabric. The PDA/Fe/HDS PET fabric was immersed in 30 g L^{-1} NaCl solution prepared by grade III water at a bath ratio of 1 : 50 for 30 min, and the excess solution was squeezed out, and the fabric (40 ± 2 mm × 100 ± 2 mm) was placed between acrylic-resin plates (60 mm × 115 mm × 1.5 mm) to withstand 12.5 ± 9 kPa pressure, then kept it in a 37 ± 2 °C oven for 4 h, 8 h, 12 h, 16 h, 20 h and 24 h. The stability of seawater resistance was characterized by the changes of WCA and SA.

The pH and organic solvents stability tests

The PDA/Fe/HDS PET fabric was immersed in different pH solutions of 1, 3, 5, 7, 9, 11 and 13 for 24 h to evaluate the pH stability, and immersed in carbon tetrachloride (CCl_4), acetone (AT), *n*-hexane (*n*-H), petroleum ether (PE), dichloromethane (DCM) and tetrahydrofuran (THF) for 72 hours to measure the organic solvent stability.

Self-cleaning property and antifouling performance test

The original PET fabric and PDA/Fe/HDS PET fabric were respectively sprinkled with methylene blue powder, and rinsed with water for comparison to test their self-cleaning performance. Droplets of water, vinegar, soy sauce and sesame oil were placed on the surface of the fabric, and WCA was tested to characterize the antifouling property of the fabric.

Oil–water separation tests

In the oil–water separation tests, the heavy oil such as CCl_4, DCM and chlorobenzene (CB) were separated by a gravity-driven separation device, and the light oil such as *n*-H and PE were separated by a self-made oil absorption bag. Oil was dyed with Oil Red O while water was dyed with Methylene Blue. For the adsorption bag oil–water separation test, the PDA/Fe/HDS PET fabric was filled with polyurethane (PU) sponge to form an oil adsorption bag.

The oil–water separation efficiency (η) is calculated according to eqn (1):

$$\eta = \left(\frac{V_0}{V_1}\right) \times 100\% \quad (1)$$

where V_0 and V_1 are the volume of water before and after the oil–water separation, respectively.

The oil–water separation capacity (c)[42,43] is calculated according to eqn (2):

$$c = \frac{M_1}{M_0} - 1 \quad (2)$$

where M_0 and M_1 are the weight of the adsorption bag before and after the oil–water separation, respectively (the original weight of the adsorption bag is about 3.07 g).

Results and discussion

Surface morphology characterization

The surface morphology of superhydrophobic material is one of the key factors affecting its wettability. Therefore, it is of great significance to study the surface morphology of polyester fabric. A field emission scanning electron microscope (FESEM) was used to observe the surface morphology of PET fabrics. It can be seen from Fig. 3a that the surface of the original PET is smooth and has a certain degree of hydrophobicity in a short period of time. The WCA is 115.1° and the water droplet completely penetrates into the original fabric (Fig. 3a) after 4 min. The surface of PET fabric remains smooth after HDS finishing (Fig. 3b), and the WCA reached 145.2°. After finishing with PDA/

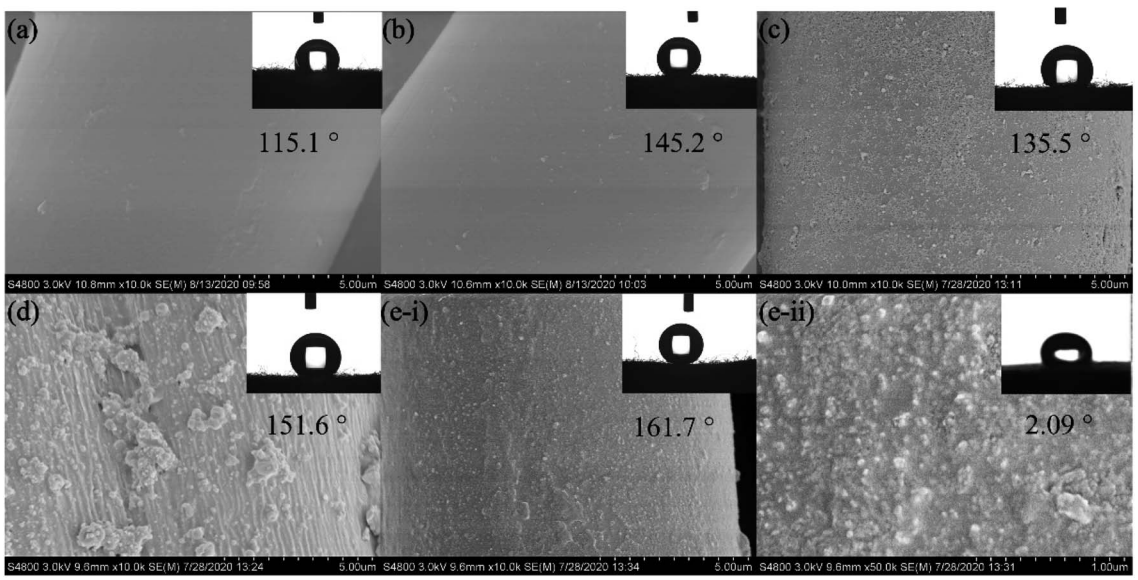

Fig. 3 SEM images of original PET fabric (a), HDS PET fabric (b), PDA/Fe PET fabric (c), PDA/HDS PET fabric (d) and PDA/Fe/HDS PET fabric (e) with different multiples, the insets are WCA (a, b, c, d and e(i)) and SA (e(ii)).

Fe (Fig. 3c) and PDA/HDS (Fig. 3d), a layer of fine nano-particles appear on the surface of the fabric, with WCA of 135.5° and 151.6°, while WCA and SA of PDA/Fe/HDS PET fabric can reach 161.7° (Fig. 3e(i)) and 2.09° (Fig. 3e(ii)), respectively. The results show that the material with low surface energy has a greater influence on the preparation of superhydrophobic polyester fabric, and the roughness can further improve the superhydrophobic property.

Atomic Force Microscopy (AFM) was used to further characterize the surface roughness of different PET fabrics. It can be seen from Fig. 4 that the original PET fabric and HDS PET fabric have smooth surfaces, the root mean square (RMS) value of the smooth original PET fabric surface and HDS PET fabric were approximately 4.16 nm and 4.04 nm. The higher RMS value represents larger roughness.[44] Compared with the original PET fabric, the rough structure of PDA/Fe PET fabric covered by the nano particles can be clearly seen from Fig. 4c, and the RMS value is about 18.63 nm. After modified with HDS, the RMS value of PET fabric is further increased to 44.38 nm (Fig. 4d). The PDA/Fe PET fabric and PDA/Fe/HDS PET fabric have rough surfaces, which are consistent with the results of SEM. Therefore, the presence of PDA and metal ions can effectively increase the surface roughness of the fabric. By increasing the surface roughness of the PET fabric while reducing the surface energy, a superhydrophobic PET fabric with good hydrophobic properties can be prepared.

Chemical analysis of PDA/Fe/HDS PET fabric

The chemical structure and chemical compositions of the fabric are mainly determined by FTIR and XPS analysis. Table 1 lists the element compositions of different PET fabrics obtained by XPS. The original PET fabric contains carbon (68.34%) and oxygen (31.66%) elements. After HDS finishing, a layer of long-chain alkyl siloxane is deposited on the surface of the PET fabric, the carbon element content is increased to 79.13%, and 3.36% silicon element is introduced. The N element on the surface of the fabric treated with PDA/HDS and PDA/Fe comes from PDA. Because a large number of phenolic hydroxyl groups in PDA molecular structure can couple with HDS, the content of silicon element is increased. PDA/Fe/HDS PET fabric contains nitrogen, iron and silicon. Among them, Fe comes from metal salt and silicon comes from HDS. Fig. 5 shows the EDS distribution mapping of surface elements of PDA/Fe/HDS PET fabric. It can be seen that C and O elements are widely distributed on the surface, while N, Fe and Si elements are less, but the distribution is very uniform,[45,46] indicating that metal and HDS were successfully introduced to the PET fabric surface through dopamine.

Table 1 Surface elemental compositions of PET fabrics

	Atomic percentage of surface element (%)				
Samples	C	N	O	Fe	Si
Original PET fabric	68.34	—	31.66	—	—
HDS PET fabric	79.13	—	17.51	—	3.36
PDA/Fe PET fabric	73.07	2.68	23.68	0.56	—
PDA/HDS PET fabric	75.34	1.38	18.7	—	4.57
PDA/Fe/HDS PET fabric	81.02	1.09	10.98	0.29	6.62

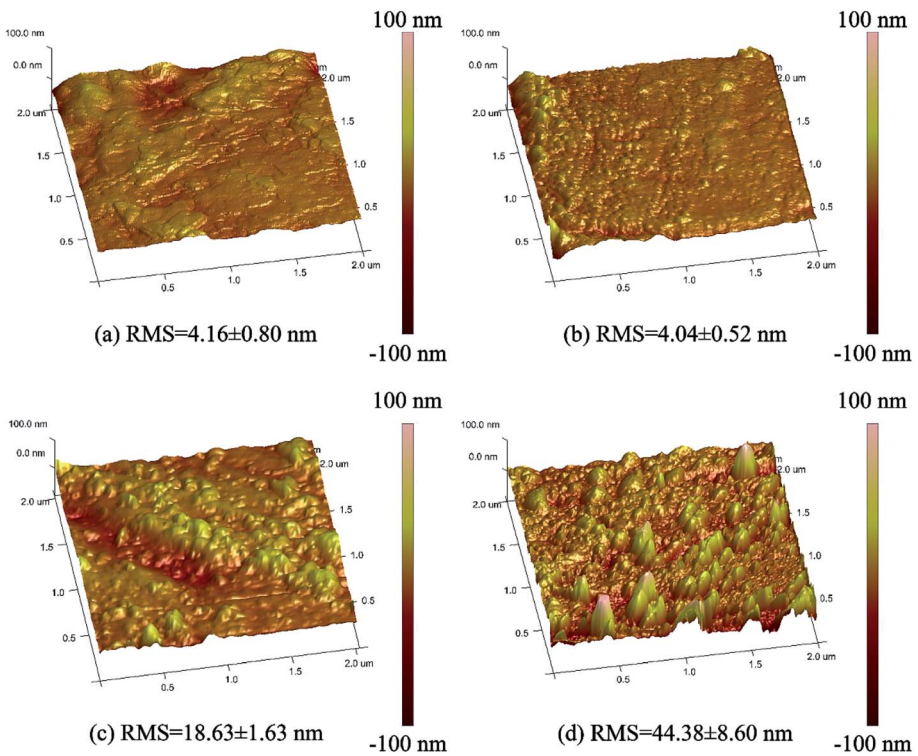

Fig. 4 AFM image of original PET fabric (a), HDS PET fabric (b), PDA/Fe PET fabric (c), and PDA/Fe/HDS PET fabric (d).

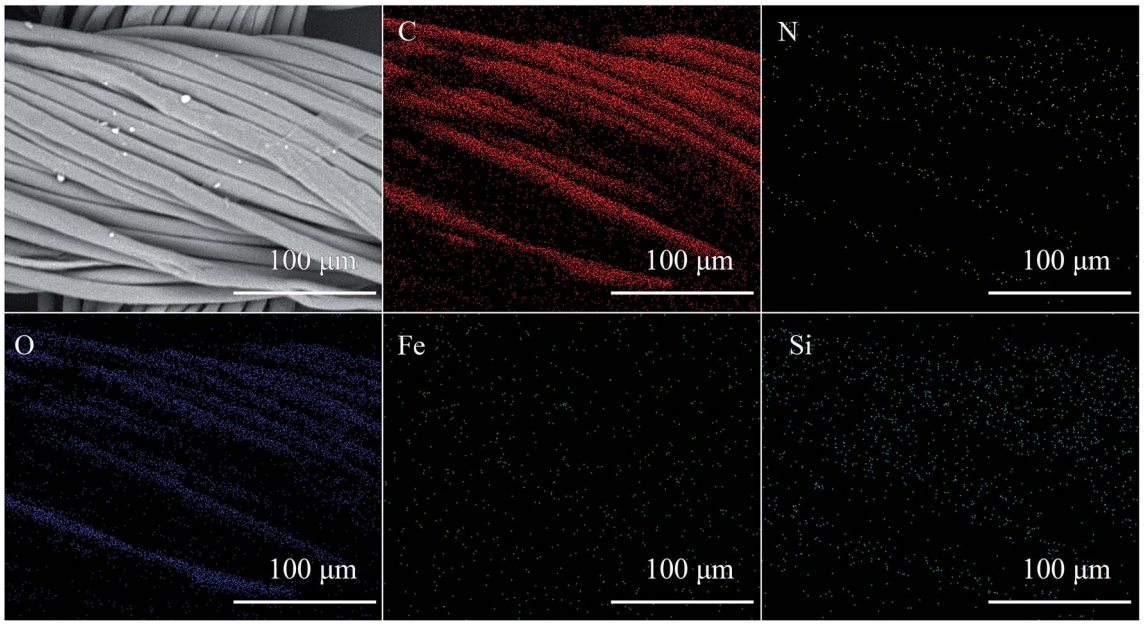

Fig. 5 Surface elemental compositions map of PDA/Fe/HDS PET fabric.

Fig. 6a shows the FTIR spectra of PET fabrics. The peak at 3311 cm^{-1} is the stretching vibration of –OH and the stretching vibration of $–NH_2$. For the spectra of HDS PET fabric, PDA/HDS PET fabric and PDA/Fe/HDS PET fabric, 2917 cm^{-1} and 2850 cm^{-1} are the symmetrical vibrations and asymmetrical stretching vibrations of $–CH_3$ and $–CH_2$ groups. The stretching vibration at 1711 cm^{-1} corresponds to C=O, which increases after the introduction of PDA due to the oxidation of the phenolic hydroxyl group in DA molecular structure to carbonyl groups. The –O=C–O vibration absorption bands of aromatic esters appear at 1245 cm^{-1} and 1094 cm^{-1}, and the peak at 1016 cm^{-1} (ref. 47) corresponds to the in-plane bending vibration of the benzene ring and the antisymmetric stretching of Si–O–Si, and the C–C and Si–O–Si symmetric stretching vibration of the aromatic rings appear at 872 cm^{-1} (ref. 48–50), indicating that the long-chain alkyl groups were successfully introduced to the surface of PET.

Fig. 6b shows the wide scan of XPS spectra of different PET fabrics, and the introduction of Si element can be seen. Due to the low content of Fe and N, there is no peak in the wide scan spectra. Fig. 7a, b and c correspond to the C1s spectra of the original PET fabric, HDS PET fabric and PDA/Fe/HDS PET fabric, and the peaks at 285.1 eV, 286.7 eV, 288.9 eV and 290.1 eV correspond to C–C/C–H, C–O, C=O and O–C=O bonds,[50,51] respectively. The new peak at 285.7 eV corresponding to C–N bond appears in Fig. 7c. Fig. 7d and e are the N1s spectrum and Fe2p spectrum of PDA/Fe PET fabric, respectively. In Fig. 7d, the peaks at 399.7 eV, 402.4 eV and 398.5 eV correspond to –NH–, $–NH_2$ and –N= bonds. The –N= bond may be derived from the intramolecular rearrangement of PDA. In Fig. 7e, Fe2p peaks appear at 727.3 eV and 713.4 eV. Fig. 7f shows the Si2p spectrum of PDA/Fe/HDS PET fabric, and three peaks at 103.8 eV, 102.6 eV and 101.9 eV belong to C–Si–O–Si, C–Si–O–H and C–Si–O–C bonds.[52,53] The results of XPS and FTIR confirmed that Fe^{2+} and HDS were successfully co-deposited on the surface of PET fabric through the strong adhesion of PDA.

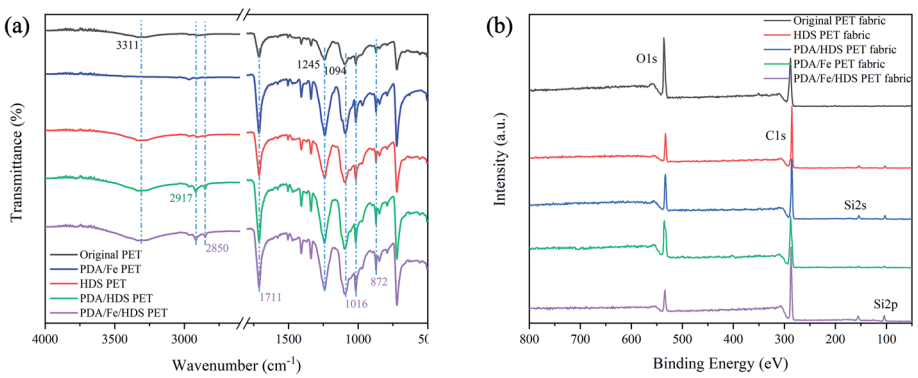

Fig. 6 The FTIR patterns (a) and wide scan XPS (b) spectra of PET fabrics.

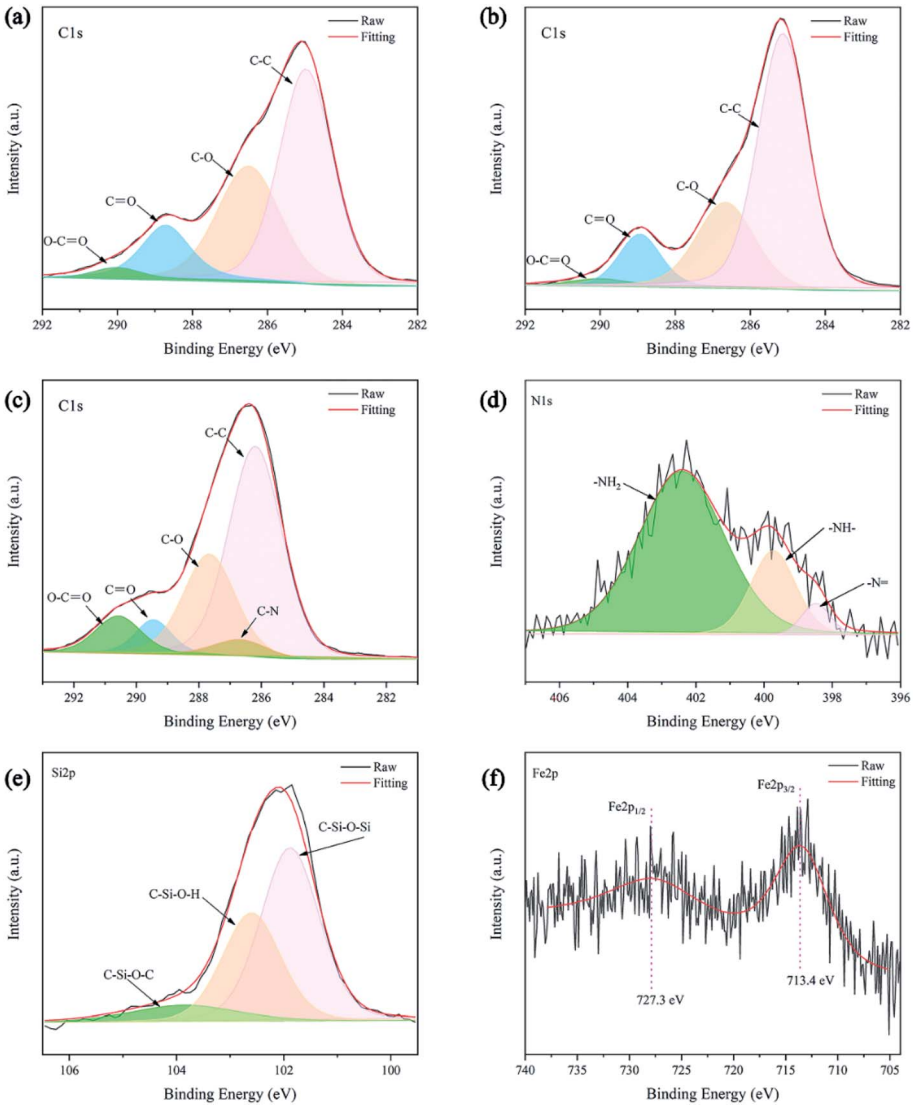

Fig. 7 XPS C1s spectra of the original PET fabric (a), HDS PET fabric (b) and PDA/Fe/HDS PET fabric (c); XPS N1s (d) and Fe2p (e) spectra of PDA/Fe PET fabric; XPS Si2p spectra of PDA/Fe/HDS PET fabric (f).

Mechanical stability of PDA/Fe/HDS PET fabric

The biggest advantage of PET fabric is its good wrinkle resistance and shape retention. Therefore, the change of strength before and after modification is also one of the important indexes of its stability. Table 2 lists the breaking strength and elongation at break before and after superhydrophobic finishing. The results show that the strength of PET fabric before and after superhydrophobic finishing has almost no change, indicating that this modification method is mild and has little effect on the mechanical properties of the fabric, and the fabric is not easy to be damaged during use.

Stability tests of the PDA/Fe/HDS PET fabric

The complexity of the marine environment requires the superhydrophobic materials used for oil–water separation to have certain physical/chemical stability and durability in harsh

Table 2 Mechanical properties of original PET fabric and PDA/Fe/HDS PET fabric

Property	Original PET fabric	PDA/Fe/HDS PET fabric
Breaking strength (N)	586.99 ± 12.68 (warp) 419.49 ± 12.49 (weft)	577.48 ± 16.67 (warp) 421.44 ± 14.13 (weft)
Elongation at break (%)	14.18 ± 1.01 (warp) 16.75 ± 0.53 (weft)	14.19 ± 0.48 (warp) 16.99 ± 0.66 (weft)

environments. Accordingly, the physical stability of fabrics was tested, including washing fastness, abrasion resistance and UV aging resistance, and the chemical stability mainly includes seawater resistance, acid and alkali resistance and organic reagent resistance (Fig. 8).

The washing fastness is one of the most important tests for fabric finishing. The washing stability test was done according to AATCC 61-2006 standard method, which is equivalent to 5 laundering cycles of commercial and domestic washing.[21] WCA and SA of the superhydrophobic PET fabric prepared after washing at 0 min, 45 min, 90 min, 135 min, 180 min, and 225 min were tested, respectively. After washing, WCA of the PDA/Fe/HDS PET fabrics are still stable above 150°, and SA remains at about 10° (Fig. 8a). Due to the strong adhesion of PDA, after 5 laundering cycles, the staining fastness of cotton and polyester is about level 5, and the fading fastness of modified fabric remained level 4.5.

After 0, 200, 400, 600, 800 and 1000 cycles of abrasion, WCA and SA of the fabrics were tested. The results showed that with the increase of abrasion cycles, the fluff on the surface of the fabric increased, WCA of the fabric gradually decreased, and SA gradually increased (Fig. 8b). However, WCA of the washed fabrics are all greater than 150° and SA are less than 10°, which remained in the superhydrophobic range. WCA and SA of PDA/Fe/HDS PET fabric were measured after being exposed to the Accelerated Weathering Tester UV for 4 h, 8 h, 12 h, 16 h, 20 h and 24 h at 60 °C to simulate the effect of sunlight on superhydrophobic properties of PDA/Fe/HDS PET fabric in outdoor oil–water separation or outdoor storage. The results are shown in Fig. 8c, the WCA of PET fabric has little change after 24 h of

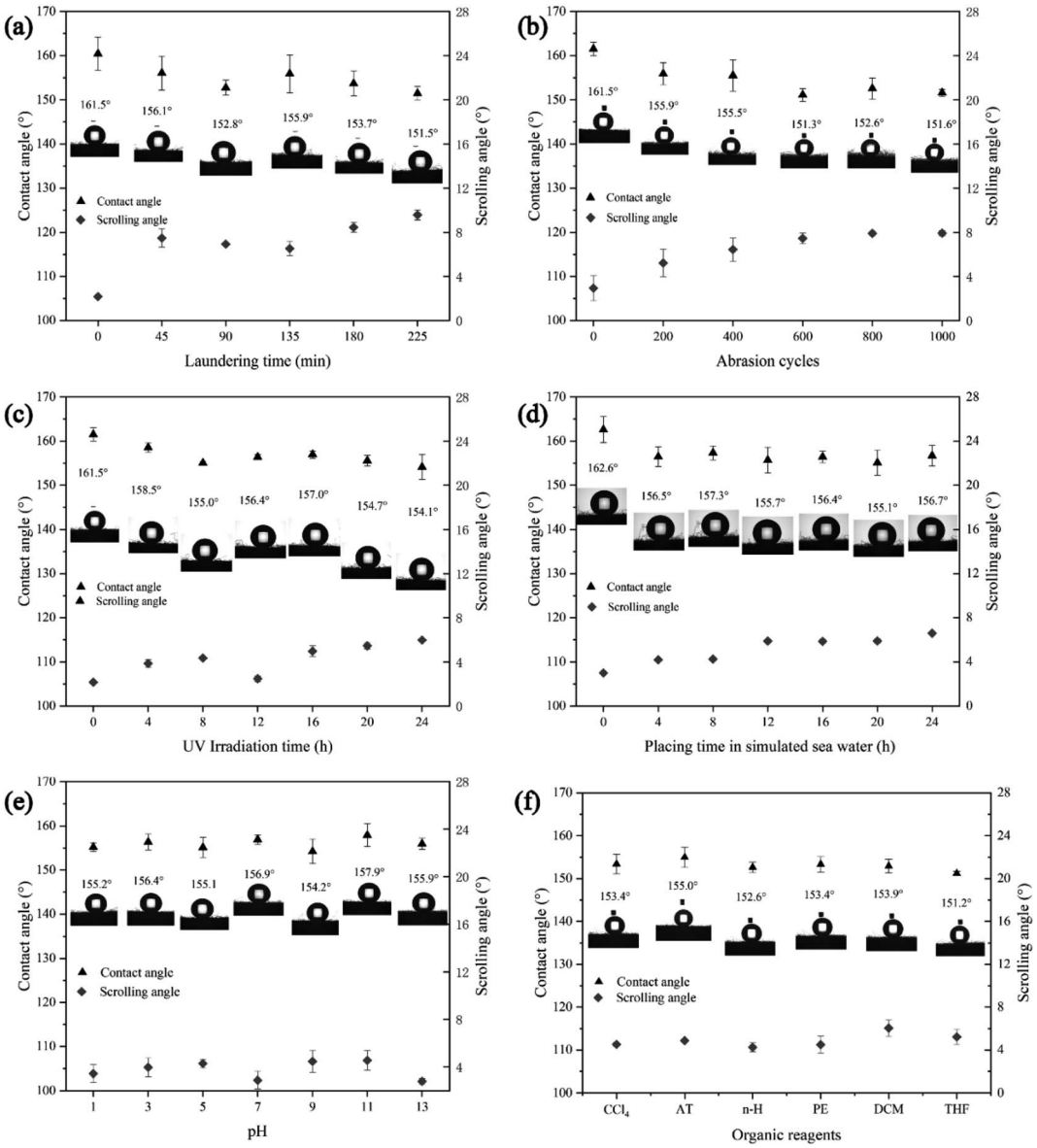

Fig. 8 The stability of PDA/Fe/HDS PET fabric with washing resistance (a), abrasion resistance (b), UV aging resistance (c), seawater resistance (d), acid/alkali resistance (e) and organic reagents resistance (f).

UV irradiation, indicating that the fabric has good stability and resistance to ultraviolet radiation.

Due to the potential application of superhydrophobic PET fabric in marine oil spill accidents and the complexity of marine environment, it is very important to test its stability against seawater, acid/alkali and organic reagents. The PDA/Fe/HDS PET fabric was placed between acrylic-resin plates to withstand 12.5 ± 9 kPa pressure for several hours to test its durability in the sea. The results are shown in Fig. 8d, the lowest WCA decreased to 155.1°, and the fabric shows good stability against seawater erosion. The fabric was soaked in a solution of pH 1, 3, 5, 7, 9, 11, 13 prepared by HCl and NaOH for 24 hours to test the acid and alkali resistance of the superhydrophobic properties of PDA/Fe/HDS PET fabric. The data (Fig. 8e) shows superhydrophobic property of the fabrics change little in different pH solutions. The WCAs were above 155°, and SA were about 10°. The organic solution stability tests can simulate the stability of superhydrophobic materials to various adsorbed marine oils. The PDA/Fe/HDS PET fabrics were soaked in CCl_4, AT, *n*-H, PE, DCM and THF for 72 h, respectively. The changes of WCA and SA were tested to characterize the stability of the fabric against organic reagents. The result shows that WCA of the soaked fabrics are above 150°, and the SA are about 10° (Fig. 8f). The WCA decreased by about 10° compared with that before soaking, which may be due to the fact that part of HDS was dissolved in the organic solvents, which increased the surface energy of the fabric and destroyed the superhydrophobic property.[54,55] It can be seen from the stability test results that the prepared superhydrophobic PET fabric has excellent resistance to washing, abrasion, UV irradiation, sea water, acid/alkali and organic reagents, which provides basis for its application in oil/water separation.

Self-cleaning property and antifouling performance test of PDA/Fe/HDS PET fabric

The methylene blue dye was sprayed randomly on the surface of the fabric, and the water droplets mixed the dye quickly on the surface of original PET fabric and contaminated the sample (Fig. 9a). The water droplets on the surface of PDA/Fe/HDS PET fabric quickly rolled off and took away the dye, and the mixed solution flowed into the culture dish, leaving a clean and flawless sample surface (Fig. 9b).

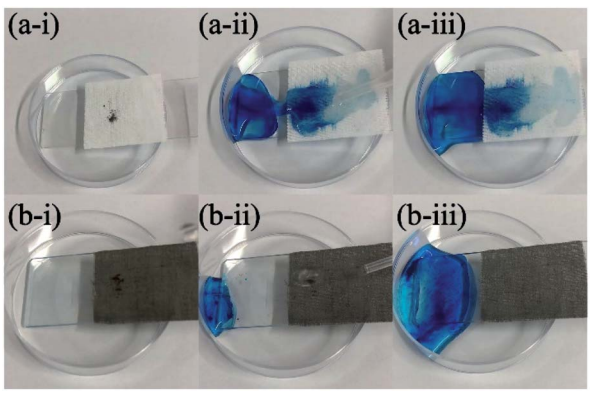

Fig. 9 Self-cleaning performance of original PET fabric (a), and PDA/Fe/HDS PET fabric (b).

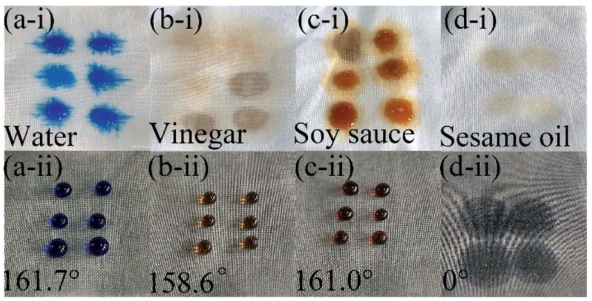

Fig. 10 Droplets of water, vinegar, soy sauce and sesame oil on the original PET fabric (a(i), b(i), c(i) and d(i)) and PDA/Fe/HDS PET fabric (a(ii), b(ii), c(ii) and d(ii)).

The fabricated superhydrophobic PET fabric shows excellent self-cleaning performance like a lotus leaf.

Water, vinegar, soy sauce and sesame oil were dropped on the surface of the prepared superhydrophobic PET fabric. After testing, the WCA of water, vinegar and soy sauce on the surface of the sample are 161.7°, 158.6° and 161.0°, respectively (Fig. 10a(ii)–c(ii)), while the sesame oil penetrates directly into the sample (Fig. 10d(ii)). The results show that PDA/Fe/HDS PET fabric has excellent antifouling, hydrophobic and lipophilic properties.

Oil–water separation properties

With the advance of industrialization, a large amount of oily wastewater generated in the production process. To explore the oil absorption function of the superhydrophobic fabric, the modified fabric (4 cm × 4 cm) was used to adsorb organic reagents (*n*-H and DCM) from water to prove that the superhydrophobic fabric can remove oil stains from water. As shown

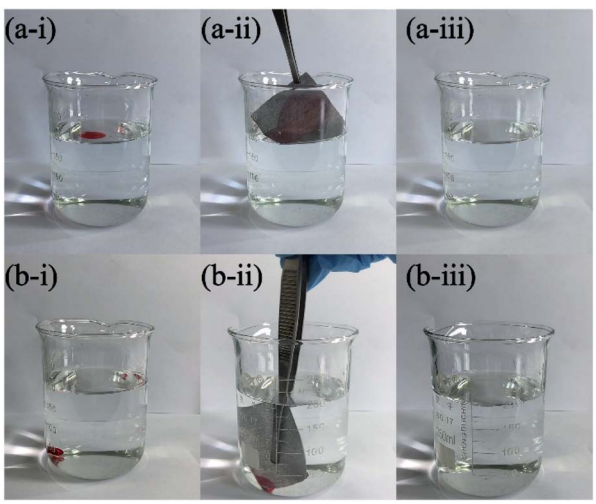

Fig. 11 Selective absorption of modified fabric for (a) *n*-H and (b) DCM (dyed with Oil Red O) in water.

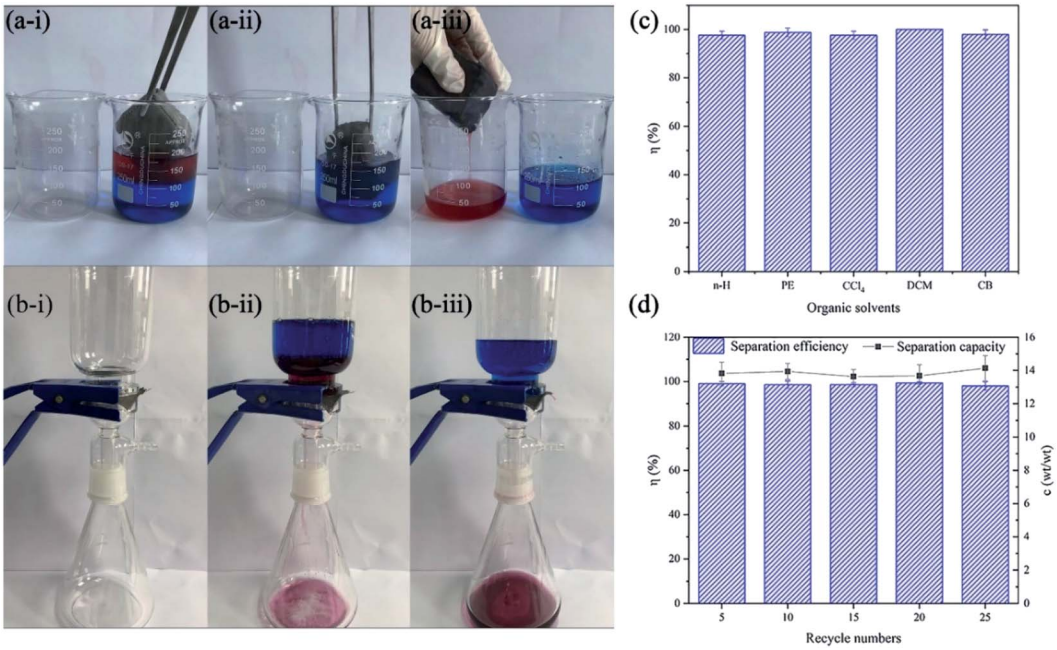

Fig. 12 The adsorption bag for light oil/water separation (a), and gravity-driven oil–water separation device (b); the separation efficiency (η) of PDA/Fe/HDS PET fabric or adsorption bag for different organic solvent (c), and the recycle numbers of recyclability (d).

in Fig. 11, the modified PET fabric can adsorb a small amount of light oil *n*-H (Fig. 11a) and heavy oil DCM (Fig. 11b) in water.

In the separation process of light oil/water mixture, 80 mL of *n*-H or PE was mixed with 100 mL of water to simulate the state of floating oil at sea. To improve the oil adsorption capacity of PDA/Fe/HDS PET fabric, a self-made oil absorption bag containing three-dimensional porous PU nanosponge was made. The results show (Fig. 12a) that the experimental oil is quickly absorbed and the volume of water remains unchanged. The prepared oil adsorption bag has excellent adsorption capacity, which can absorb light oil about 14 times of its own weight (Fig. 12d). The adsorption capacity depends on the size of the oil adsorption bag and sponge, and its size is adjustable.

The heavy oil/water mixture was separated by gravity driven method (Fig. 12b). The target heavy oil such as CCl_4, DCM and CB were marked with Red Oil O, and the water was marked with methylene blue. The PDA/Fe/HDS PET fabric was fixed on the glass device, and then 200 mL of oil/water mixture was poured. Due to the excellent hydrophobic and lipophilic properties of the fabric, the oil soaked the fabric and entered the flask and the water was retained. The separation efficiency is about 99% (Fig. 12c). After 5, 10, 15, 20, and 25 times of separation, the separation efficiency is still above 95% (Fig. 12d), therefore, it is considered that PDA/Fe/HDS PET fabric has good application value in oil–water separation.

Conclusions

In this work, superhydrophobic PDA/Fe/HDS PET fabric was successfully fabricated. The excellent adhesion property of PDA contributes to the fastness of HDS on PET fabric, thereby greatly reducing the surface tension of the fabric, resulting in a superhydrophobic PET fabric with WCA up to 161.7° and SA about 2.09°. Compared with the traditional preparation method of oil–water separation material, this method is simple, the reagents used are environmentally friendly, and the reaction time is greatly shortened. The amount of HDS and the cost of the substrate were both reduced, and the prepared superhydrophobic fabrics had good stability against various harsh environments and excellent reusability. This work opens up a new way to expand the value of PET fabrics and inspires the practical the practical application of durable superhydrophobic fabrics.

Conflicts of interest

There are no conflicts to declare.

Acknowledgements

This work was supported by the National Natural Science Foundation of China (51973144, 51741301); the Major Program of Natural Science Research of Jiangsu Higher Education Institutions of China (18KJA540002); the Foundation of Jiangsu Engineering Research Center of Textile Dyeing and Printing for Energy Conservation, Discharge Reduction and Cleaner Production (Q811580621); the Priority Academic Program Development (PAPD) of Jiangsu Higher Education Institutions for Textile Engineering in Soochow University.

References

1 J. Ou, F. Wang, W. Li, M. Yan and A. Amirfazli, *Prog. Org. Coat.*, 2020, **146**, 105700.
2 X. Zhang, F. Shi, J. Niu, Y. Jiang and Z. Wang, *J. Mater. Chem.*, 2008, **18**, 621–633.

3 S. Rezaei, I. Manoucheri, R. Moradian and B. Pourabbas, *Chem. Eng. J.*, 2014, **252**, 11–16.
4 Q. Zhou, B. Yan, T. Xing and G. Chen, *Carbohydr. Polym.*, 2019, **203**, 1–9.
5 B. Yan, Q. Zhou, T. Xing and G. Chen, *Polymers*, 2018, **10**, 128316.
6 F. F. Chen, Y. J. Zhu, Z. C. Xiong, T. W. Sun and Y. Q. Shen, *ACS Appl. Mater. Interfaces*, 2016, **8**, 34715–34724.
7 F. Abdelghaffar, R. A. Abdelghaffar, U. M. Rashed and H. M. Ahmed, *Environ. Sci. Pollut. Res.*, 2020, **27**, 28949–28961.
8 S. Zhu, Z. Kang, F. Wang and Y. Long, *Nanotechnology*, 2021, **32**, 035701.
9 X. Wang, Y. Lu, Q. Zhang, K. Wang, C. J. Carmalt, I. P. Parkin, Z. Zhang and X. Zhang, *J. Colloid Interface Sci.*, 2021, **582**, 301–311.
10 C. H. Xue, X. Q. Ji, J. Zhang, J. Z. Ma and S. T. Jia, *Nanotechnology*, 2015, **26**, 335602.
11 T. He, X. Chen, Y. Wang, Z. Cheng, Y. Liu, X. Wang, L. Luo, Y. Chen and X. Liu, *Appl. Surf. Sci.*, 2020, **515**, 146006.
12 K. Liu, K. Qi, Y. Zhao, X. Wang, C. Yang, J. Fu, Y. Li and P. Li, *Mater. Lett.*, 2020, **263**, 127237.
13 A. B. Gurav, Q. Guo, Y. Tao, T. Mei, Y. Wang and D. Wang, *Mater. Lett.*, 2016, **182**, 106–109.
14 M. Z. Khan, J. Militky, V. Baheti, M. Fijalkowski, J. Wiener, L. Voleský and K. Adach, *Cellulose*, 2020, **27**, 10519–10539.
15 C. H. Xue, X. J. Guo, M. M. Zhang, J. Z. Ma and S. T. Jia, *J. Mater. Chem. A*, 2015, **3**, 21797–21804.
16 J. H. Oh, T. J. Ko, M. W. Moon and C. H. Park, *RSC Adv.*, 2017, **7**, 25597–25604.
17 T. Anupriyanka, G. Shanmugavelayutham, B. Sarma and M. Mariammal, *Colloids Surf., A*, 2020, **600**, 124949.
18 J. Zhang, J. Zhao, W. Qu, X. Li and Z. Wang, *J. Colloid Interface Sci.*, 2020, **580**, 211–222.
19 Y. Chen, X. Wu, J. Wei and H. Wu, *Macromol. Mater. Eng.*, 2020, **305**, 1–10.
20 D. Cheng, Y. Zhang, X. Bai, Y. Liu, Z. Deng, J. Wu, S. Bi, J. Ran, G. Cai and X. Wang, *Cellulose*, 2020, **27**, 5421–5433.
21 X. Dong, S. Gao, J. Huang, S. Li, T. Zhu, Y. Cheng, Y. Zhao, Z. Chen and Y. Lai, *J. Mater. Chem. A*, 2019, **7**, 2122–2128.
22 L. Chen and Z. Guo, *Colloids Surf., A*, 2018, **554**, 253–260.
23 Q. Lin, D. Gourdon, C. Sun, N. Holten-Andersen, T. H. Anderson, J. H. Waite and J. N. Israelachvili, *Proc. Natl. Acad. Sci. U. S. A.*, 2007, **104**, 3782–3786.
24 J. Yu, Y. Kan, M. Rapp, E. Danner, W. Wei, S. Das, D. R. Miller, Y. Chen, J. H. Waite and J. N. Israelachvili, *Proc. Natl. Acad. Sci. U. S. A.*, 2013, **110**, 15680–15685.
25 W. Wei, J. Yu, C. Broomell, J. N. Israelachvili and J. H. Waite, *J. Am. Chem. Soc.*, 2013, **135**, 377–383.
26 J. Yu, W. Wei, E. Danner, R. K. Ashley, J. N. Israelachvili and J. H. Waite, *Nat. Chem. Biol.*, 2011, **7**, 588–590.
27 Z. A. Levine, M. V. Rapp, W. Wei, R. G. Mullen, C. Wu, G. H. Zerze, J. Mittal, J. H. Waite, J. N. Israelachvili and J. E. Shea, *Proc. Natl. Acad. Sci. U. S. A.*, 2016, **113**, 4332–4337.
28 J. N. Israelachvili, *Biomacromolecules*, 2013, **14**(4), 1072–1077.
29 S. Li, C. Wang, T. Wang, Q. Wang and X. Zhang, *J. Appl. Polym. Sci.*, 2020, **137**, 1–9.
30 H. Lee, S. Dellatore, W. Miller and P. Messersmith, *Science*, 2007, **318**, 426.
31 W. Wang, Y. Jiang, Y. Liao, M. Tian, H. Zou and L. Zhang, *J. Colloid Interface Sci.*, 2011, **358**, 567.
32 H. Kang, X. Song, Z. Wang, W. Zhang, S. Zhang and J. Li, *ACS Sustainable Chem. Eng.*, 2016, **4**, 4354.
33 Z. Wang, Y. Xu, Y. Liu and L. Shao, *J. Mater. Chem. A*, 2015, **3**, 12171–12178.
34 J. Wang, Y. Chen, Q. Xu, M. Cai, Q. Shi and J. Gao, *Sci. Rep.*, 2021, **11**, 1–17.
35 D. Hong, K. E. Bae, S. P. Hong, J. H. Park, I. S. Choi and W. K. Cho, *Chem. Commun.*, 2014, **50**, 11649–11652.
36 S. Y. Lee, J. H. Park, M. Yang, M. J. Baek, M. H. Kim, J. Lee, A. Khademhosseini, D. D. Kim and H. J. Cho, *Int. J. Pharm.*, 2020, **582**, 119309.
37 T. An, N. Lee, H. J. Cho, S. Kim, D. S. Shin and S. M. Lee, *RSC Adv.*, 2017, **7**, 30582–30587.
38 Y. Sun, A. N. Pham and T. D. Waite, *J. Neurochem.*, 2016, 955–968.
39 P. J. Babu, S. Saranya, A. M. Raichur and M. Doble, *Mater. Lett.*, 2020, **277**, 128316.
40 N. F. Della Vecchia, R. Avolio, M. Alfè, M. E. Errico, A. Napolitano and M. D'Ischia, *Adv. Funct. Mater.*, 2013, **23**, 1331–1340.
41 C. Lim, J. Huang, S. Kim, H. Lee, H. Zeng and D. S. Hwang, *Angew. Chem., Int. Ed.*, 2016, **55**, 3342–3346.
42 Z. Li and Z. Guo, *Mater. Des.*, 2020, **196**, 109144.
43 G. Huang, B. Lai, H. Xu, Y. Jin, L. Huo, Z. Li and Y. Deng, *Sep. Purif. Technol.*, 2021, **258**, 118063.
44 C. Cao, M. Ge, J. Huang, S. Li, S. Deng, S. Zhang, Z. Chen, K. Zhang, S. S. Al-Deyab and Y. Lai, *J. Mater. Chem. A*, 2016, **4**, 12179–12187.
45 S. Kumar, M. M. Rahman, S. Yoon, S. Kim, N. Oh, K. H. Hong and J. Koh, *Fibers Polym.*, 2021, 1–11.
46 X. Chen, R. Chu, T. Xing and G. Chen, *Colloids Surf., A*, 2021, **611**, 125803.
47 F. Zhou, Y. Zhang, D. Zhang, Z. Zhang, F. Fu, X. Zhang, Y. Yang, H. Lin and Y. Chen, *Colloids Surf., A*, 2021, **609**, 125686.
48 S. S. Ray, Y. I. Park, H. Park, S. E. Nam, I. C. Kim and Y. N. Kwon, *Environ. Technol. Innovation*, 2020, **20**, 101093.
49 Y. Cai, Q. Zhao, X. Quan, W. Feng and Q. Wang, *Colloids Surf., A*, 2020, **586**, 124189.
50 M. N. Morshed, M. Asadi Miankafshe, N. K. Persson, N. Behary and V. A. Nierstrasz, *Dalton Trans.*, 2020, **49**, 17281–17300.
51 S. Xiao, P. Xu, Q. Peng, J. Chen, J. Huang, F. Wang and N. Noor, *Polymers*, 2017, **9**, 735.
52 A. A. Nimbekar and R. R. Deshmukh, *J. Mater. Sci.: Mater. Electron.*, 2021, **32**, 59–72.
53 Z. Zhang, H. Liu and W. Qiao, *Colloids Surf., A*, 2020, **589**, 124433.
54 Y. Cai, Q. Zhao, X. Quan, W. Feng and Q. Wang, *Colloids Surf., A*, 2020, **586**, 124189.
55 P. Zhang, S. Dong, B. Li, X. Wei and J. Zhang, *Appl. Clay Sci.*, 2018, **157**, 237–247.